Characterization of Technetium-99m-L,L-ECD for Brain Perfusion Imaging, Part 2: Biodistribution and Brain Imaging in Humans

Jean Léveillé, Georges Demonceau, Michael De Roo, Pierre Rigo, Raymond Taillefer, Robert A. Morgan, Donna Kupranick, and Richard C. Walovitch

Department of Nuclear Medicine, Hôtel-Dieu de Montréal, Montréal, Canada; Department of Nuclear Medicine, University of Liege, Liege, Belgium; Department of Nuclear Medicine, Universitaire Ziekenhuizen, Leuven, Belgium; and Diagnostics Division-Imaging Agents, E. I. Du Pont de Nemours & Co. (Inc.), N. O. Billerica, Massachusetts

The safety, biodistribution and kinetics of a new perfusion imaging agent [^{99m}Tc-L,L]-ethyl cysteinate dimer (ECD) was evaluated in normal volunteers. Technetium-99m-L,L-ECD is a neutral, lipophilic complex, which is radiochemically pure and stable. Twelve healthy adults were injected with 25–30 mCi of ^{99m}Tc-L,L-ECD and imaged periodically for up to 24 hr. Planar imaging showed rapid brain uptake with a peak concentration of 4.9% injected dose and very slow brain washout (~6% per hour during the first 6 hr). Repeat or dynamic tomographic imaging of the brain using either a rotating gamma camera or a multidetector system was performed up to 6 hr postinjection. The distribution of ^{99m}Tc-L,L-ECD in the brain did not change and was similar to the pattern seen with other perfusion agents. Background facial areas and lungs cleared rapidly. Peak blood activity was below 10% injected dose at all times and ^{99m}Tc-L,L-ECD cleared rapidly through the kidneys. Vital signs, blood and urine chemistries were normal in all volunteers and no adverse reactions were noted. These results suggest that ^{99m}Tc-L,L-ECD should be useful for routine assessment of cerebral perfusion in humans.

J Nucl Med 30:1902–1910, 1989

Understanding of the complete diagnostic and prognostic value of brain perfusion imaging to the general nuclear medicine community requires the development of radiopharmaceuticals that are readily available and are compatible with existing rotating single photo emission computed tomography (SPECT) instrumentation.

The first agents of this type were the iodine-123- (^{123}I) labeled amines: ^{123}I-labeled iodoamphetamine (IMP Spectamine, Medi-Physic, Inc., Emeryville, CA), and ^{123}I-N,N,N,'-trimethyl-N'-(2-hydroxyl-3-methyl-5-iodo-benzyl)-1,3-propane diamine (HIPDM) (*1*). However, these tracers have several disadvantages. First, the radioisotopic characteristics of ^{123}I are not optimal for routine use. Its 13 hr half-life limits radioactive dose that can be injected to under 5 mCi (*2,3*). Since ^{123}I is not generator produced and because of its short physical half-life, it is difficult to transport long distances to outlying hospitals. Thus, the radiopharmaceutical is not readily available for many potential applications. Another concern is that brain distribution of IMP changes over time (*4,5*). This causes the quality of the perfusion image to degrade such that by an hour postadministration, the brain distribution no longer represents perfusion at the time of injection (*6*).

Recently, work has begun on the development of technetium-99m (^{99m}Tc) -labeled agents to obviate some of the disadvantages of iodinated amines. The first compound to be widely evaluated was ^{99m}Tc-HM-PAO (Amersham Inc., Ltd., Amersham UK), HM-PAO, a d,l-diastereoisomer of hexamethyl-propyleneamine oxime, forms a neutral complex with ^{99m}Tc which distributes relative to rCBF (*7*). However, chemical decomposition of [^{99m}Tc]HM-PAO begins shortly after it is prepared so that the time available between reconstitution of the kit and injection of the ^{99m}Tc complex is limited to 30 min (*8*).

Received Feb. 7, 1989; revision accepted July 24, 1989.

For reprints contact: Jean Léveillé, MD, Département de Médicine Nucléaire, Hôtel-Dieu de Montréal; 3840 Rue St.-Urbain; Montréal, Québec, Canada H2W 1T8.

The results of a study to evaluate the safety and pharmacokinetics of the chemically stable complex, ^{99m}Tc-ethyl cysteinate dimer (^{99m}Tc-L,L-ECD), in eight normal male volunteers using dynamic planar, whole-body, and SPECT imaging are reported here. In addition, four normal volunteers were studied using a multicrystal dynamic SPECT camera to determine neuroanatomical information on ^{99m}Tc-L,L-ECD localization and to obtain dynamic SPECT analysis from relatively pure gray and white matter zones.

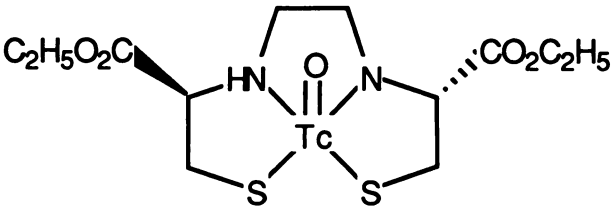

FIGURE 1
Structure of ^{99m}Tc-L,L-ethyl cyteinate dimer (^{99m}Tc-L,L-ECD).

MATERIALS AND METHODS

Preparations of the ^{99m}Tc-L,L-ECD complex (Fig. 1) were made at both Hôtel-Dieu de Montréal, Canada (volunteer Group A) and the University of Liege, Belgium (volunteer Groups B and C).

A total of 0.9 mg of the ligand N,N'-1,2-ethanediylbis-L-cysteine diethylester dihydrochloride (ECD·2HCl, Wellcome Foundation Ltd., Temple Hill, Dartford, UK) with 72 μg $SnCl_2 \cdot 2H_2O$, 360 μg Na2EDTA·$2H_2O$ and 24 mg mannitol was dispensed and lyophilized in a 5 ml vial (Vial A). Another vial (Vial B) contained 1 ml of 0.0187*M* phosphate buffer (pH 7.5) under air. To form the ^{99m}Tc-L,L-ECD complex, saline (1.2 ml) was injected into the first vial containing the ECD and the vial was shaken to dissolve the contents. One milliliter of the solution was withdrawn by syringe and injected into the buffer vial. Technetium-99m generator eluate (25–50 mCi) was added to Vial B and then reacted at room temperature for at least 15 min prior to administration.

Following the reconstitution of the kits with ^{99m}Tc, the radiochemical purity of the final complex was determined using thin layer chromatography (TLC) on Whatman MKC18 plates, developed with acetone: 0.5*M* ammonium acetate (60:40). The plates were scanned using a gamma camera and the activity ratios were determined by comparing the main peak $R_f = 0.35$ with the sum of all other peaks. All kits used had radiochemical purity >95%. Chromatographic results obtained from kits up to 6 hr postreconstitution were identical to those obtained at injection time and confirmed the stable and pure labeling of ECD with ^{99m}Tc.

Subjects

A total of 12 normal volunteers (nine males, three females; 21–58 yr) were evaluated in this study. Eight of the volunteers were studied using rotating SPECT gamma cameras while four were evaluated using MD-SPECT. Each volunteer was required to pass a medical examination and to have a negative neurologic evaluation prior to participating in the study. Written informed consent was obtained from each volunteer, and the protocol had been reviewed and accepted by the institutional review board of both hospitals.

^{99m}Tc-L,L-ECD Imaging Protocols

Group A consisted of four normal male volunteers (Subjects 1–4) who were studied in Montréal, Canada: Group B (Subjects 5–8) consisted of four normal male volunteers who were studied in Liege, Belgium. Dynamic planar brain images were acquired in Groups A and B, followed by repeat SPECT and repeat whole-body planar spot imaging as outlined in Figure 2. Clinical chemistries, urinalysis, hematology and venous blood activity of ^{99m}Tc-L,L-ECD also were obtained in each volunteer.

In both Groups A and B, a catheter was inserted into the volunteer's antecubital arm vein opposite the arm to be used for the injection of the radiopharmaceutical and a baseline blood sample was drawn. Each volunteer then was positioned supine with the orbito-meatal line (OML) perpendicular to the axis of rotation and with the gamma camera in the anterior or lateral orientation. The volunteer was allowed to acclimate to the imaging room with eyes open and ears unplugged for at least 15 min prior to initiation of the study. The imaging room was dimly lit and quiet except for machine background noise. Technetium-99m-L,L-ECD (28–30 mCi) was injected directly in an antecubital vein followed by a 5–10 ml saline flush. Dynamic planar imaging began immediately using a 64 × 64 word-mode matrix and 1 min per frame data acquisition for 20 min. Rotating gamma camera SPECT imaging was initiated within 5 min following the completion of the dynamic planar imaging study. SPECT data was collected into 64 × 64 word mode matrices using angular increments of 3° over 360°. A minimum of 60,000 counts per view, restricted by an acquisition time not exceeding 20 sec per view, was obtained. Four anterior whole-body spot images were used to evaluate the biodistribution of ^{99m}Tc-L,L-ECD starting at 90 min postinjection. The SPECT imaging and anterior whole-body spot imaging sequence were performed again at ~240

Groups A & B

Minutes Post-injection	
0–20	Dynamic Planar Anterior or Lateral Imaging 1 min/view, 64 x 64 Matrix
21–73	SPECT 2.8–3.0° View For 360° 17–20 sec/view, 64 x 64 Matrix
75–90	Four Anterior Body Spots 300,000 Counts or 3 min/view
100–153	Repeat SPECT
155–170	Repeat Body Spot Images
240	Repeat SPECT and Body Spot Images
360	Repeat SPECT and Body Spot Images
1440	Repeat Whole Body Spot Images
	GROUP C
0–60	MD-SPECT at 4.5 and 7 cm Above OML Alternating Levels Every 4 min
70–180	Step-up Views 4 min Each 1.5 cm/slice

FIGURE 2
Protocols for image acquisition in each volunteer group following injection of ^{99m}Tc-L,L-ECD.

and 360 min postinjection. At 1440 min postinjection, another set of anterior spot images were acquired.

In Group A, scintigraphic acquisition and processing were performed on a Picker Dyna Digital Camera (Picker International, Highland Heights, OH) equipped with a square SX-300 detector and a low-energy, high resolution collimator. An energy setting of 140 keV with a 15% window was used.

Group B was studied on a General Electric GE400-AT camera interfaced to a Star Computer (General Electric Company, Milwaukee, WI). The camera was equipped with a low-energy, all purpose collimator on volunteers 5 and 6 and a high resolution collimator was used on volunteers 7 and 8. An energy setting of 140 keV with a 15% window was used.

Group C (Subjects 9–12) consisted of four volunteers (three females, one male) studied at Leuven, Belgium. Multidetector SPECT imaging was performed at two levels of the brain over the first hour following the injection of ^{99m}Tc-L,L-ECD using a NOVO 810 instrument (Novo Diagnostic Systems, Bagsvaerd, Denmark). Step through images from the base to the vertex of the brain were obtained during the second hour postinjection (Fig. 2). Brain tomograms (1.5 cm slices, parallel to the OML) also were obtained for anatomic comparison to MD-SPECT images. The volunteer was positioned and acclimated as previously stated. Using an antecubital vein, 30 mCi of ^{99m}Tc-L,L-ECD was injected followed by a 5–10 ml saline flush. Beginning immediately and continuing for 1 hr, alternating single-slice, 4-min images were collected at ~4.5 and then 7.0 cm above the OML. Between 1 and 1.5 hr postinjection, a series of 4-min tomographic images were obtained representing a 1.5 cm per slice stepwise progression through the brain from the base to the vertex.

Statistical Analysis

All values in the text are means plus or minus s.e.m. Statistical significance of ^{99m}Tc-L,L-ECD dynamic planar brain clearance and washout from blood cells, as compared with hematocrit standards are determined by Freedman nonparametric analysis of variance (ANOVA) (*9*). Two-way ANOVA with repeated measures was used to compare the territorial clearance of ^{99m}Tc-L,L-ECD in five brain regions during the different SPECT studies. Three-way ANOVA with repeated measures was performed to determine washout of ^{99m}Tc-L,L-ECD from head regions of interest during SPECT acquisition periods.

Safety Data

Blood pressure, pulse, respiration, and temperature were measured immediately prior to the injection of ^{99m}Tc-L,L-ECD and periodically for up to 24 hr postinjection. Blood and urine samples also were collected immediately prior to and periodically after injection for up to 24 hr. These samples were used to monitor changes in clinical chemistries (SMA 12 or equivalent) and to allow for the determination of percent injected dose (% ID) of ^{99m}Tc-L,L-ECD in blood and urine. In Group A, the distribution of ^{99m}Tc-L,L-ECD in the blood also was determined following centrifugation.

Image Data Analysis—Groups A and B

In Groups A and B, camera calibration was performed before each study. The center of rotation offset, the pixel dimension, and the camera efficiency were determined the day before each study.

The % ID in the brain was determined from the initial 20 min dynamic images and the anterior whole-body spot images. A region of interest (ROI) encompassing only the brain, excluding as much scalp and facial activity as possible, was drawn; and the count rate in the brain versus time was obtained. ROIs defining facial glandular structures were used to monitor changes in background activity. Decay corrected count rates were converted to percent ID in the brain by utilizing the gamma camera counting efficiency that had been determined from a 1000 ml polystyrene phantom containing a calibrated amount of ^{99m}Tc. This method was also used to determine the percent ID in the other various body organs.

Transaxial, sagittal, and coronal tomographic images were generated using filtered backprojection. The raw data from the rotating gamma camera was prefiltered using a commercially available prereconstruction, two-dimensional Fast Fourier Transform or a 9-point convolution filter, then backprojected using a ramp filter. There was no postreconstruction image filtering. The rotating gamma camera tomographic images were corrected for attenuation uniformity, and deviation from the center of rotation.

Territorial ROIs were drawn according to von Schulthess (*10*) on selected transaxial or coronal images that contained representative territories supplied by the anterior, middle, or posterior cerebral arteries or the area of the basal ganglia and cerebellum (Fig. 3A). A comparison was done between the results obtained with one slice (6 mm/slice) and the successive addition of two, three, and four slices together. The appropriate transaxial or coronal slices were divided into nonoverlapping and symmetric ROIs that represented the territories within that slice. Both hemispheres were studied simultaneously at 20, 100, 240, and 360 min postinjection. Data from each volunteer were normalized to 100% maximum activity set on the mean counts per pixel from the first SPECT acquisition.

Technetium-99m-L,L-ECD clearance was determined from different head regions during a SPECT acquisition using ROI analysis of planar projections. Regions of constant size and shape were drawn on uniformity-corrected planar projections of each SPECT study for all eight volunteers. The first three and last three planar projections (20 sec/projection) of each SPECT study were used for analysis. Mean activity per pixel in all ROIs were decay-corrected and normalized to activity per pixel of the first three planar projections from the first SPECT study. The elapsed time between the first and last planar projections was ~50 min.

Image Data Analysis—Group C

Transaxial slices generated on the multidetector camera were used to evaluate the gray to white matter ratios over time. Representative gray and white ROIs were drawn on slices obtained 7 cm above the OML with gray matter regions defined in the left and right frontal and left and right occipital lobes and compared with those of adjacent left and right periventricular white matter regions (Fig. 3B). Relative concentrations of activity in left to right (mean activity/pixel) ratios in the frontal (using 7.0 and 4.5 cm slice) and occipital corticies (7.0 cm slice) were also determined.

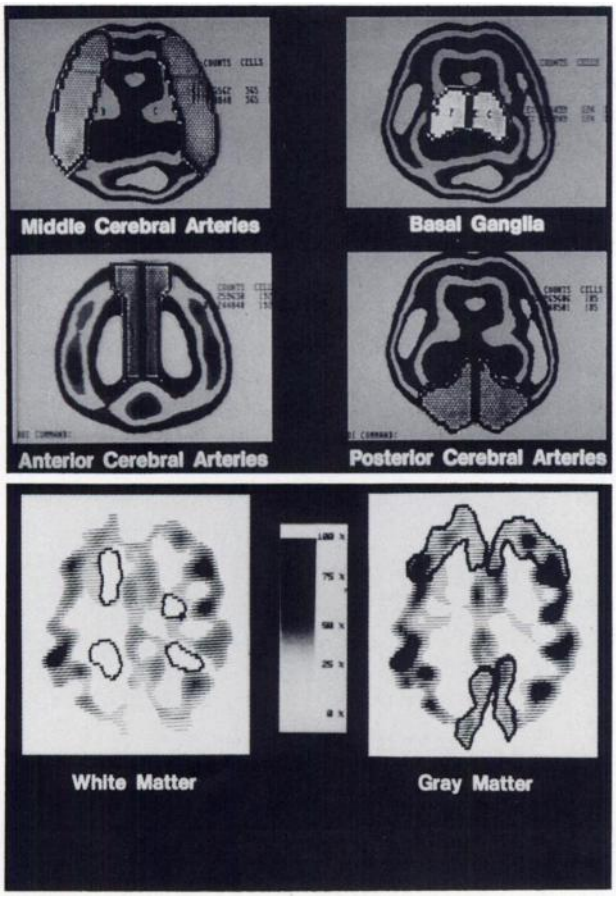

FIGURE 3
Brain tomographic ROI. All rotating gamma camera SPECT ROIs are nonoverlapping and were drawn on 2.4-cm slices (3A). MD-SPECT brain images (7 cm above the OML 1 hr post-^{99m}Tc-L,L-ECD administration) show representative gray and white matter ROIs (3B).

RESULTS

Blood and Urine Studies

No significant changes in the blood cell counts or blood or urine chemistries were observed throughout the study. All vital signs were stable and unchanged, and no adverse reaction was observed during any study.

The rapid clearance of ^{99m}Tc-L,L-ECD from the blood is illustrated in Figure 4. Technetium-99m-L,L-ECD activity peaks at 7–8% ID between 5–20 min postadministration and then drops to 4% by 1 hr and under 2% by 2 hr postinjection. The relative distribution of ^{99m}Tc-L,L-ECD in blood plasma and red blood cells (RBC) was determined in the venous blood samples of four volunteers (Group A). The results (Fig. 5) show that ^{99m}Tc-L,L-ECD initially partitions equally in total cellular and plasma fractions. Thus the concentration of activity in the cellular fraction was the same as the hematocrit. However, by 5 min postinjection, a disproportionate amount of activity was in the plasma ($p > 0.05$ for all times from 5–60 min). This, combined with the rapid blood clearance of ^{99m}Tc-L,L-ECD, suggests that it does not bind strongly to blood cells or plasma proteins.

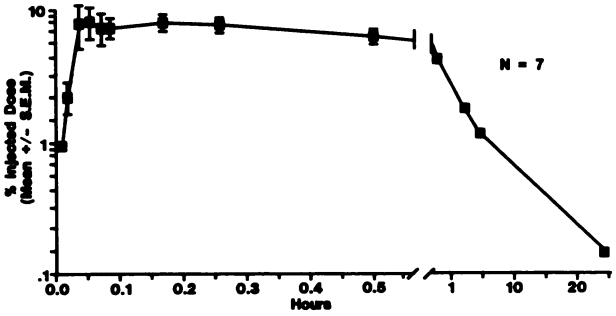

FIGURE 4
Venous blood clearance of ^{99m}Tc-L,L-ECD in seven normal adult males. All values are mean ± s.e.m. % ID

Technetium-99m-L,L-ECD was cleared rapidly via renal excretion. At 2 hr postinjection 55% ± 10 % ID was eliminated. Cumulative urinary excretion of 78% ± 14 % ID was obtained by 24 hr.

Dynamic Planar Brain Imaging Studies

Brain dynamic planar imaging studies show ^{99m}Tc-L,L-ECD to be rapidly extracted by brain tissue (Fig. 6). No difference in brain kinetics or initial % ID were observed between the anterior and lateral view acquisitions. No washout of activity from the brain was observed during the initial 20 min imaging study ($p > 0.05$). Figure 7 shows the clear delineation of the cortical gray and white matter structures even in planar acquisition and the rapid washout of activity from background facial areas and lung.

Static Planar Imaging

Figure 8 shows the selective brain retention of ^{99m}Tc-L,L-ECD in eight normal males. It was not possible to

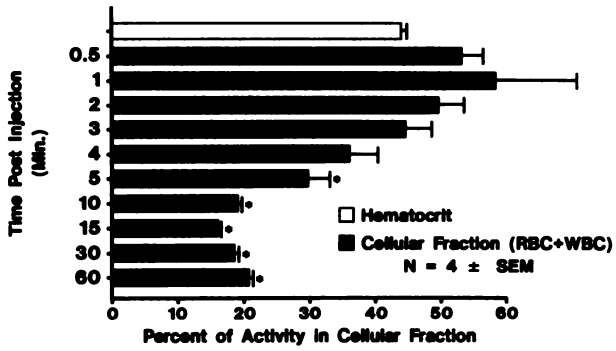

FIGURE 5
Percent of total ^{99m}Tc-L,L-ECD blood activity in the red blood cells (RBC) and white blood cells (WBC). All values are mean ± s.e.m. from four normal adult males. Cellular retention was determined by centrifuging venous blood samples and determining the ratio of activity between the cellular and plasma fractions. Significant clearance from the cellular fraction ($p < 0.05$) was observed starting at 5 min postadministration of ^{99m}Tc-L,L-ECD when compared to the mean hematocrit value.

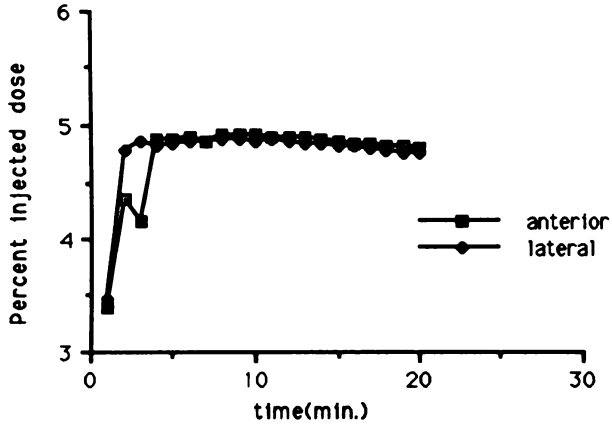

FIGURE 6
Dynamic planar brain time-activity curve showing the rapid uptake and stable brain concentration of ^{99m}Tc-L,L-ECD during the first 20 min postadministration. Each point represents the mean ± s.e. of six normal males studied from the lateral view and two from the frontal.

determine an accurate whole brain $T_{1/2}$ due to the small number of time points and their distribution (no time points earlier than 90 min were taken). Technetium-99m-L,L-ECD brain washout is slow enough that it would not in itself be a practical limitation in doing an imaging study a few hours postadministration.

No statistically significant differences in the brain, liver, gallbladder, or lung time-activity curves were observed between Groups A and B. Minor, but potentially clinically significant, differences in the initial uptake in the lungs were different for the two groups. The initial lung % ID was higher in Group B, which was composed of three smokers (4.42 ± 2.03) as compared to Group A which was composed of four nonsmokers (1.36 ± 0.80). The one nonsmoker in Group B (Volunteer 7) had a 90 min lung % ID of 2.8. However, in both Groups A and B, the lungs, similarly to the blood, cleared rapidly. This suggests that shortly after ^{99m}Tc-L,L-ECD administration little activity remains available for uptake into the brain.

Clearance kinetics appeared to be similar in both Group A and B for all organs studied. The delay peak in the gallbladder activity is attributed to hepatobiliary clearance of the compound. The intestinal elimination of ^{99m}Tc-L,L-ECD is relatively small compared with the predominate renal excretion.

Rotating SPECT Studies

High resolution SPECT images of greater than 4,500,000 counts per study were obtained for up to 7 hr postadministration of 28–30 mCi of ^{99m}Tc-L,L-ECD (Fig. 9). Qualitatively, the reconstructed SPECT images demonstrate excellent differentiation between gray and white matter structures at all times postinjection. The low background activity greatly enhances the clarity of these images, particularly in the coronal presentation. Reconstructed images of between 0.6 and 2.4 cm in coronal, sagittal and transverse planes demonstrated that the ^{99m}Tc-L,L-ECD distribution pattern is similar to what would be anticipated from a tracer which distributes according to rCBF.

Quantitatively, no significant regional clearance variations were observed between the five brain territories (territories of the anterior, middle and posterior cerebral arteries, the basal ganglia and the cerebellum, Fig. 10A). All areas showed less than a 30% clearance between the first and the 6-hr SPECT study. Changing the slice thickness from 0.6 cm to 2.4 cm had no effect on these results. Left/right asymmetry of activity was <5% in all areas. In all studies, the highest tracer uptake was found in the occipital region.

The study of clearance during a brain SPECT acquisition in the eight normal males showed that there was significant difference in ^{99m}Tc-L,L-ECD clearance when the brain regions (left and right hemispheres) were compared to background regions (scalp and neck), however, all regions appear to show a monoexponential rate of clearance (i.e., first scan versus last scan) (Fig. 10B). All main effects and interaction terms (head ROIs changes over time during a SPECT acquisition and changes between SPECT studies) were significant at $p < 0.001$.

During the first SPECT study, the left hemispheric clearance was 5 ± 2% and the right hemispheric clearance was 7 ± 1%. Simple main effects showed that there was no significant difference in the rate of clearance between the left and right hemispheres during any of the SPECT studies. During the first SPECT study a significantly greater decrease in activity was observed in the scalp and neck (24 ± 13% and 45 ± 9%, respectively) as compared with either the left or right hemisphere.

The neck and lower face clearance appears to have little or no effect on the apparent overall brain clearance. The rate of clearance in the lower part of the brain (<5 cm above OML) where the facial glandular and neck contribution would be greatest was no different than clearance rates from the upper part of the brain (>5 cm above OML) (data not shown).

Multidetector SPECT Studies

Qualitatively, the MD-SPECT reconstructed images show the same good gray to white matter differentiation and distribution pattern that was observed in the rotating gamma camera SPECT images. Distribution of ^{99m}Tc-L,L-ECD in the brain was unchanged over time. In the step-through imaging studies performed between 1 and 3 hr postinjection, all gray matter areas had high uptake of ^{99m}Tc-L,L-ECD. The higher resolution of the imaging system compared to rotational SPECT cameras, allows for the greater differentiation and more

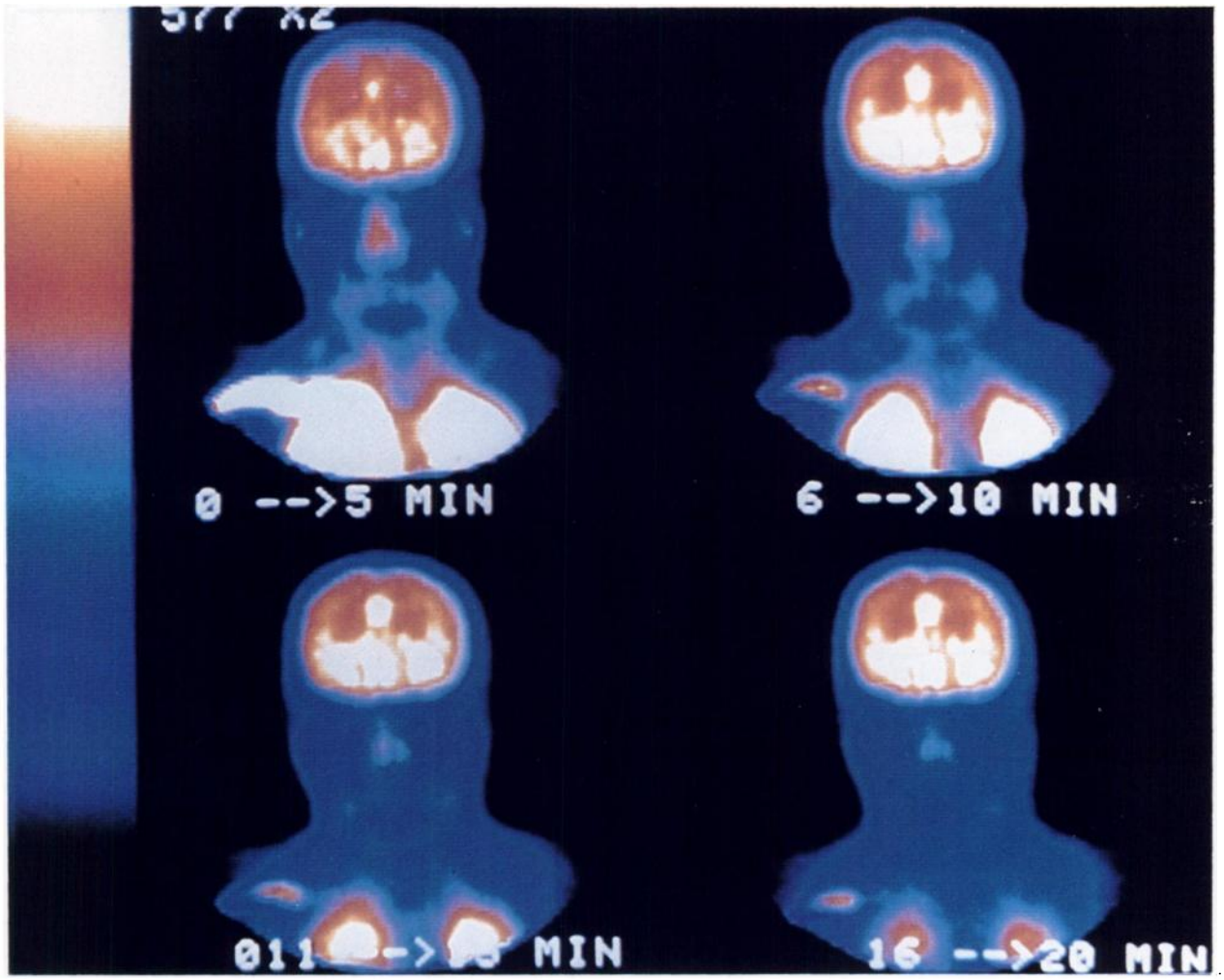

FIGURE 7
Dynamic planar frontal images of a normal male. Each of the four images are sums of five, 1-min planar images. Imaging was initiated immediately after ^{99m}Tc-L,L-ECD administration. Note the delineation of the cortical gray and white matter structures and the rapid washout from background facial and lung areas.

heterogeneous appearance of the brain with resolution of sulci and gyri (Fig. 11). Quantitatively, the retention of ^{99m}Tc-L,L-ECD in the brain, as determined by total activity in the 4.5 and 7 cm slices, was less than that determined by the SPECT studies. Clearance per hour was approximately double that which was observed in the rotating SPECT study. This discrepancy can be attributed to the inclusion of non-brain counts in the total brain counts obtained from the MD-SPECT slice because of partial volume effects on image reconstruction.

Gray to white matter contrast was unchanged over time and was always greater than 2:1 (Fig. 12). Gray matter ROIs in the frontal and occipital lobes demonstrate no significant differences in ^{99m}Tc-L,L-ECD activity between the left and right hemispheres. Mean frontal gray matter asymmetry at all times postinjection was <5%.

DISCUSSION

These studies suggest ^{99m}Tc-L,L-ECD to be safe and clinically useful for brain perfusion imaging in normal volunteers. Its major advantages over other agents is that it is a ^{99m}Tc complex which can be prepared at high radiochemical purity, is radiochemically stable, and upon administration to humans, maintains a constant pattern of distribution consistent with perfusion. These characteristics will allow for flexible scheduling of patient imaging studies and should expand the diagnostic utility of brain perfusion imaging in the assessment of acute neurologic diseases (e.g., acute head trauma, acute stroke, focal epilepsy). The superior photon flux of ^{99m}Tc, as compared to ^{123}I, will allow for higher resolution imaging in a shorter acquisition time. This should be amenable for use in uncooperative patients (e.g., demented or psychiatric patients).

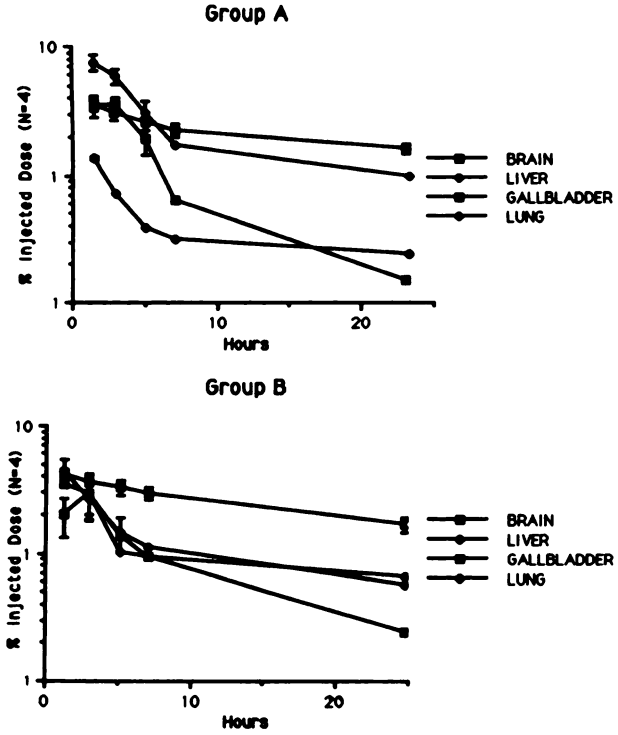

FIGURE 8
Whole-body biodistribution of ^{99m}Tc-L,L-ECD in two groups of four normal male adults. All values are mean ± s.e.m. Both groups show the brain selective retention of ^{99m}Tc-L,L-ECD. Three of the four volunteers in Group B were smokers and had elevated lung % ID values.

FIGURE 9
Rotating gamma camera transverse SPECT images of a normal adult man. SPECT imaging was performed 100 min after administration of ^{99m}Tc-L,L-ECD.

The pharmacokinetics of ^{99m}Tc-L,L-ECD are close to optimal for brain perfusion imaging. It washes out much more slowly from the brain than any other organ (Fig. 5). Clearance is rapid from all nonbrain areas of the head and the blood. This results in excellent contrast between brain and adjacent tissue when performing planar imaging (Fig. 7). The rapid blood clearance and minor lung retention of this agent also contributes to the excellent image quality of ^{99m}Tc-L,L-ECD by eliminating any pool of activity that might continue to supply activity to the brain.

The brain pharmacokinetics of ^{99m}Tc-L,L-ECD are complex. Brain clearance of between 5–6% is observed during the first rotating SPECT study (20–70 min post-injection). During this same time period, scalp and neck activity decreases by 24–45%, respectively.

The rotational SPECT and MD-SPECT studies show the ^{99m}Tc-L,L-ECD brain distribution pattern to be unchanged over time and to be similar to the distribution pattern observed with other SPECT perfusion agents. Although ^{99m}Tc-L,L-ECD showed significant brain clearance between the early and late SPECT studies, the rate of clearance was the same in all brain areas. If ^{99m}Tc-L,L-ECD brain clearance was flow dependent, one would expect ^{99m}Tc-L,L-ECD to clear at a faster rate from higher flow brain areas. Even the high flow gray matter brain regions cleared at the same rate as low flow white matter brain areas (Fig. 12). This suggests that the brain clearance of ECD is not related primarily to flow.

The rapid clearance from facial and neck soft tissues significantly reduces radioactivity around the brain. As a consequence, the ratio of brain/soft tissue rapidly rises over time. This may make the brain more easily visualized at its base (primarily on sagittal and coronal slices) where the possible influence of activity in nonbrain structures is the greatest.

Rapid blood clearance also contributes to the good imaging quality of ^{99m}Tc-L,L-ECD. This rapid clearance with minor brain washout may prove to be important in cerebral blood flow and blood volume studies. The measurement of cerebral blood flow/blood volume has been shown to be a very sensitive indicator of vascular reserve and useful to indicate tissue ischemia (*11,12*). High circulating blood activity levels or changing brain activity may be problematic in blood flow/blood volume studies (*12–15*). The low blood concentration of ^{99m}Tc-L,L-ECD is likely to improve the ability to detect ischemia in the brain since increased blood volume due to autoregulation will have minimal effect on image quality (*16*).

Technetium-99m-L,L-ECD is rapidly cleared from the blood to the urine where the majority of the injected dose (55% ID) appears by 2 hr postinjection. These data support the non-human primate dosimetry data which determined the dose limiting organ to be the bladder wall. This is ideal for imaging since the radiation burden to the bladder can be altered by changing the voiding interval. These dosimetric characteristics are ideal to perform multiple injection studies using chemical or cognitive challenges. Such studies appear to increase the diagnostic and prognostic sensitivity of blood flow imaging for various diseases (*17,18*).

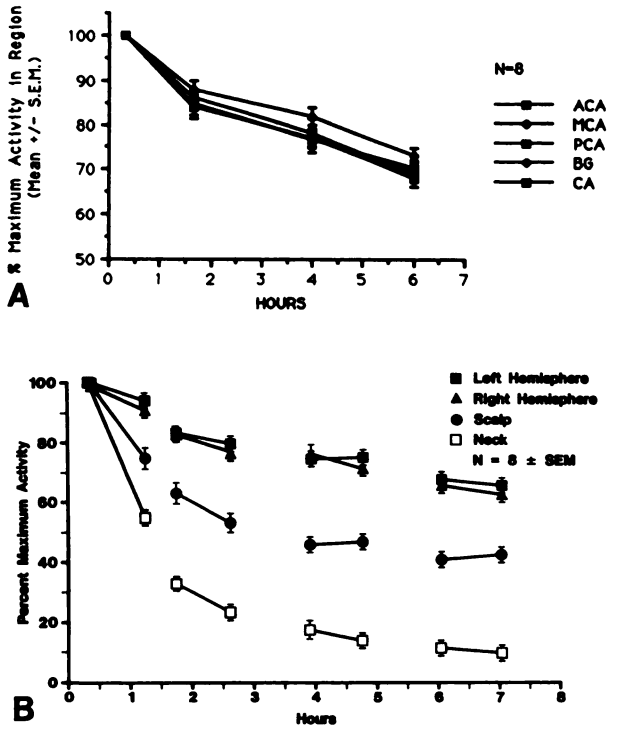

FIGURE 10
A: ^{99m}Tc-L,L-ECD regional brain SPECT clearance in five brain regions: anterior cerebral artery (ACA), posterior cerebral artery (PCA), middle cerebral artery (MCA) basal ganglia (BG) and cerebellum (CA). In this group of eight normal males, all areas showed approximately 30% clearance of ^{99m}Tc-L,L-ECD in 6 hr. Values are mean ± s.e.m. percentage of the initial activity (mean counts/pixel) in each region. No significant differences in washout were observed between the brain regions. B: ^{99m}Tc-L,L-ECD clearance during SPECT acquisition periods in eight normal males. Clearance during a SPECT acquisition was determined by comparing the mean ± s.e.m. count density in the region during the first three planar projections of the SPECT study to the mean count density during the last three views. Significant clearance was observed during all SPECT acquisition periods in both hemispheres and the neck ($p < 0.05$, except left hemisphere during third SPECT study). Clearance from the scalp was only significant during the first SPECT acquisition periods. No differences were observed between the left and right hemisphere at any times postadministration. In contrast, a much greater washout of activity ($p < 0.001$) was seen at all times postadministration in background tissues (scalp and neck) as compared to brain tissue (left and right hemisphere).

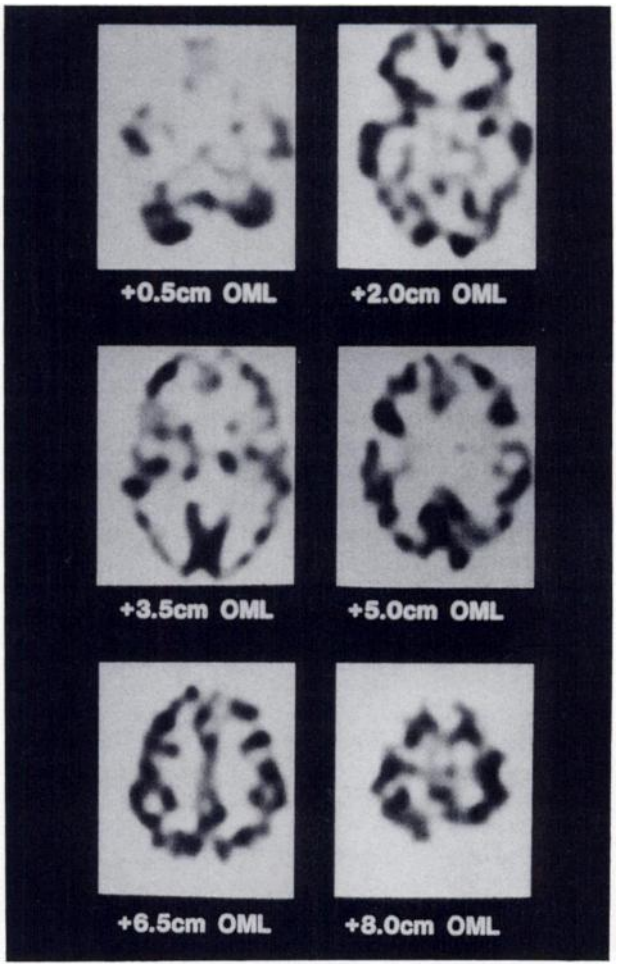

FIGURE 11
Multidetector SPECT images showing the distribution of ^{99m}Tc-L,L-ECD at six levels of the brain in a normal female. Each slice is parallel to the OML and is 1.5 cm thick. At this spatial resolution, anatomic details can be well resolved. Gyri and sulci of the cortical mantle are visible as are subcortical structures including the thalamus and caudate.

The selective brain retention and rapid clearance of ^{99m}Tc-L,L-ECD from blood through the renal system is postulated to be due to its rapid metabolism (*19–22*). Non-human primate studies suggest ^{99m}Tc-L,L-ECD to be metabolized in the brain to a polar complex which is selectively retained there. Monkey autoradiographic studies have demonstrated a close correspondence between the ^{99m}Tc brain activity and blood flow at 1 hr postadministration (*20,21*). This can be explained if diffusion, not metabolism, is the rate-limiting step for brain retention of ^{99m}Tc-L,L-ECD. Since this has only been demonstrated in nonpathologic monkey studies, it is not known if enzymatic retention may become rate limiting in different pathologies.

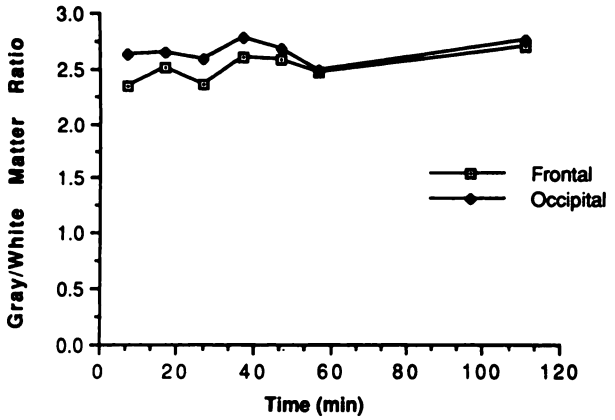

FIGURE 12
MD-SPECT cortical gray/white matter ratios for ^{99m}Tc-L,L-ECD in a normal female. Values are the mean ratios of left and right cortical activity compared to its adjacent periventricular white matter. Data was obtained using the 7 cm above OML.

In conclusion, the chemical and pharmacological characteristics of ^{99m}Tc-L,L-ECD indicate that this agent will be useful for the assessment of regional cerebral perfusion. The ease of use of ^{99m}Tc-L,L-ECD, combined with its selective brain retention and rapid renal excretion, suggest that this agent may expand the utility of perfusion imaging by presenting the physician with an agent that can be used routinely in any nuclear medicine department to determine the status of regional cerebral perfusion.

ACKNOWLEDGMENTS

The authors thank Lori Bernard for her help in collating the data, Andre Gagnon for his help in performing the imaging studies at Hôtel Dieu de Montréal and Dr. Stephen Williams for his helpful suggestions in preparing this manuscript. We also thank Jan Mosack for her invaluable secretarial assistance in the preparation of this manuscript.

REFERENCES

1. Holman BL, Hill TC. Perfusion imaging with single-photo emission computed tomography. In: Wood JM, ed. *Cerebral blood flow.* New York: McGraw-Hill, 1987:243–255.
2. Baker GA, Lum DJ, Smith EM, Winchell HS. Significance of radiocontaminants in ^{123}I for dosimetry and scintillation camera imaging. *J Nucl Med* 1976; 17:740–743.
3. Royal HD, Hill TC, Holman BL. Clinical brain imaging with isopropyl-iodoamphetamine and SPECT. *Semin Nucl Med* 1985; 15:357–376.
4. Moretti JL, Defer G, Raynaud C, et al. Early and late SPECT with N-isopropyl-P-iodoamphetamine (I-123-AMP) in cerebral ischaemia. In: Britton KE, Schmidt HAE, Ell PJ, eds. *Nuclear medicine.* Stuttgart, West Germany, Schattauer Verlag; 1986:205–209.
5. Creutzig H, Schober O, Gielow P, et al. Cerebral dynamics of N-isopropyl-(^{123}I)p-iodoamphetamine. *J Nucl Med* 1986; 27:178–183.
6. Buell U, Krappel W, Schmiedek P, et al. I-123 amphetamine vs Xe-133 SPECT. A comparative study in patients with unilateral cerebrovascular disease (CVD) [Abstract]. *J Nucl Med* 1985; 26:P25.
7. Lassen NA, Anderson AR, Friberg H, Neirinckx RD. Technetium-99m-HMPAO as a tracer of cerebral blood flow distribution: a kinetic analysis [Abstract]. *J Cereb Blood Flow Metab* 1987; 7:1,535.
8. Neirinckx R, Canning L, Piper I, et al. Technetium-99m d,l-HM-PAO: a new radiopharmaceutical for SPECT imaging of regional cerebral blood perfusion. *J Nucl Med* 1987; 28:191–202.
9. Kirk RE. Experimental design. *Procedures for the behavioral sciences.* Belmont: Brook/Cole, 1968.
10. von Schulthess GK, Ketz E, Schubiger PA, Bekier A. Regional quantitative noninvasive assessment of cerebral perfusion and function with N-isopropyl-[^{123}I] p-iodoamphetamine. *J Nucl Med* 1985; 26:9–16.
11. Levine RL. The study of cerebral ischemic reversibility: Part I. A review of positron imaging studies. *Am J Physiol Imag* 1986; 1:54–58.
12. Buell U, Braun H, Ferbert A, Stirner H, Weiller C, Ringelstein EB. Combined SPECT imaging of regional cerebral blood flow (^{99m}Tc-hexamethyl-propyleneamine oxime, HMPAO) and blood volume (^{99m}Tc-RBC) to assess regional cerebral perfusion reserve in patients with cerebrovascular disease. *Nucl Med* 1988; 27:51–56.
13. Knapp WH, von Kummer R, Kubler W. Imaging of cerebral blood flow-to-volume distribution using SPECT. *J Nucl Med* 1986; 27:465–470.
14. Knapp WH, von Kummer R, Kubler W. Reply. *J Nucl Med* 1986; 27:1939–1940.
15. Buell U, Stirner H, Ferbert F. Cerebral blood flow-to-blood volume imaging by SPECT [Letter]. *J Nucl Med* 1986; 27:1938–1939.
16. Moretti JL, Defer G, Cinotti L, Cesaro P, Vigneron N, Pethe C. Comparative tomoscintigraphic study of strokes using ECD Tc99m, HMPAO Tc99m and IMP I123. Preliminary results [Abstract]. *Eur J Nucl Med* 1988; 12:311.
17. Burt RW, Reddy RV, Mock BM, Wellman HN, Schauweeker DS, Witt R. Acetazolamide enhancement of HIPDM brain flow distribution imaging. *J Nucl Med* 1986; 27:1627–1631.
18. Weinberger DR. Schizophrenia and the frontal lobe. *Trends Neurosci* 1988; 11:367–370.
19. Walovitch RC, Hall KM, O'Toole JJ, et al. Metabolism of Tc99m-ECD in normal volunteers [Abstract]. *J Nucl Med* 1988; 29:747.
20. Walovitch R, Makuch J, Garrity S, et al. Neuropharmacological characterization of Tc99m ECD in human and non-human primates [Abstract]. *Neurol* 1988; 38:363.
21. Walovitch RC, Makuch J, Knapik G, Watson AD, Williams SJ. Brain retention of Tc99m-ECD is related to in vivo metabolism [Abstract]. *J Nucl Med* 1988; 29:747.
22. Walovitch RC, Hill TC, Garrity ST. Characterization of technetium-99m-L, L-ECD for brain perfusion imaging, Part 1: pharmacology of technetium-99m ECO in nonhuman primates. *J Nucl Med* 1989; 30:1892–1901.